



JOINT INSTITUTE FOR NUCLEAR RESEARCH

FINAL REPORT ON THE INTEREST PROGRAMME

Crystallographic texture analysis from synchrotron and neutron diffraction data

Supervisor:

Dr. Roman Vasin

Student:

Jiajia Shen, Portugal, NOVA
university of Lisbon

Participation period:

Nov 02 – Dec 12, Wave 2

Dubna, 2020

Abstract:

This project consists of three main tasks: study the basics of crystallographic texture analysis, familiarize with MAUD software, process synchrotron data of real samples to obtain textures. And the aim of this project is to learn these texture research methods and sophisticated data analysis routines. In order to achieve these goals, a combination of ODF calculation methods with a Rietveld method was performed. Specifically, we apply the MAUD software to determine the texture of the samples, and post-processing of texture data was performed using BEARTEX software with smoothing function and rotation of ODF.

In this project, three real samples, Nickel coin, NiTiZr alloy and High entropy alloy, were analyzed using a Rietveld refinement method to obtain the crystallographic texture information.

Key words: Texture analysis, ODF, Rietveld refinement.

Introduction:

Texture or crystallographic preferred orientation describes the orientation of crystallites of phases that compose a material relative to sample coordinates with a three-dimensional statistical orientation distribution function ODF, which is formed and changed by plastic deformation, sedimentation, crystallization, recrystallization, structural phase transitions¹. The texture induces anisotropy of physical and mechanical properties of the material, so the texture is not only important for mechanical properties, they are also essential for crystal structure refinements and volume fraction estimates of aggregates with preferred orientation.

Various techniques are used to determine crystallographic preferred orientations in bulk samples, most commonly X-ray, electron, and neutron diffraction. Compared with constant-wavelength neutron diffraction and electron back-scattered diffraction, high-energy synchrotron X-ray diffraction with large area detectors enables the probing of a large of crystalline orientations in individual exposures, offering the advantages of fast texture measurements^{2,3,4}. For quantitative texture analysis with high-energy simultaneous diffraction, an orientation distribution function (ODF) of textured materials is usually determined on the basis of polar pattern measurements collected as Debye-Scherrer diffraction images at different sample orientations. In such cases, Rietveld texture analysis as a method for quantitative analysis is gaining increasing researchers' attention, and have proved to be a very powerful tool for texture analysis.

This project consists of three main tasks: study texture analysis basics, familiarize with MAUD software, and process synchrotron of real samples to obtain textures. A combination of ODF calculation methods with a Rietveld method was performed, specifically, we apply the MAUD software to determine the texture of the samples, and post-processing of texture data was performed using BEARTEX software with smoothing function and rotation of ODF.

Sample 1: Nickel-coin

The schematic of the setup is shown in Figure 1. For this coin sample, which is a Cu-Ni alloy⁷, high-energy X-ray beam with short wavelength (0.10798 \AA) was used, and the distance between detector and sample is about 1850mm.

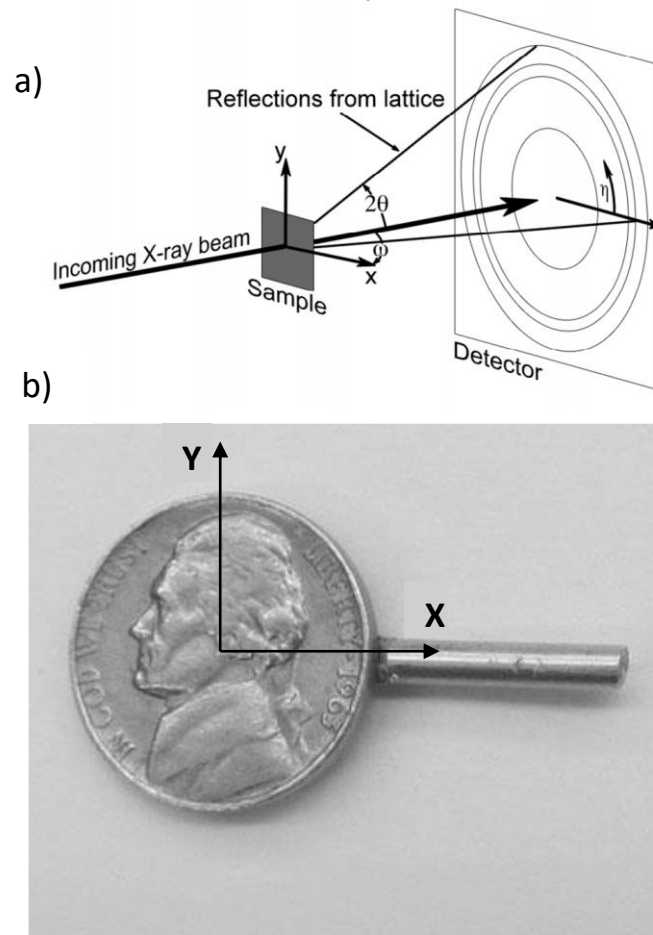


Figure 1. (a): Geometry of synchrotron diffraction texture experiment; (b): Typical sample for a hard X-ray diffraction experiment: Nickel coin mounted on a pin.

I : Instrumental Calibration

For the data refinement, it is necessary to know the instrumental parameters, such as exact sample-to-detector distance, detector center and tilt. Also, the line broadening analysis requires as a prerequisite to separate the broadening due to the sample (crystallite size and micro-strain) from the broadening arising from the instrument. The refinement strategy for the microstructure characteristics of the sample of in MAUD is different than in other Rietveld programs such as Fullprof⁵ or GSAS¹. There is a clear separation between the instrument line broadening model and the line broadening model related to the sample⁶. So using standard sample (usually powdered LaB_6 or CeO_2) to do the instrumental broadening determination is essential.

For the calibration, CeO_2 diffraction image was integrated in MAUD software in 5° azimuthal steps, and 72 diffraction patterns were simultaneously processed.

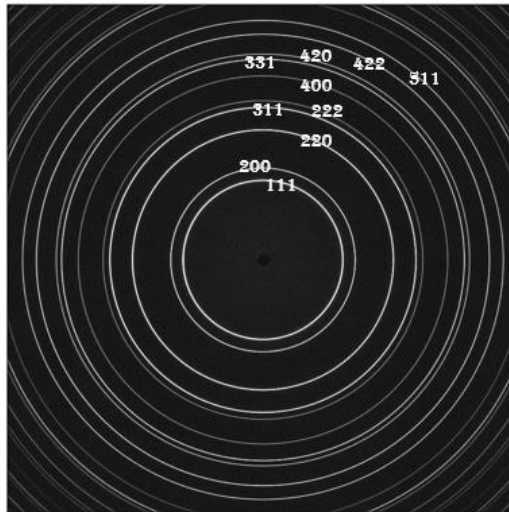


Figure 2. Diffraction image with Debye rings: CeO₂ standard.

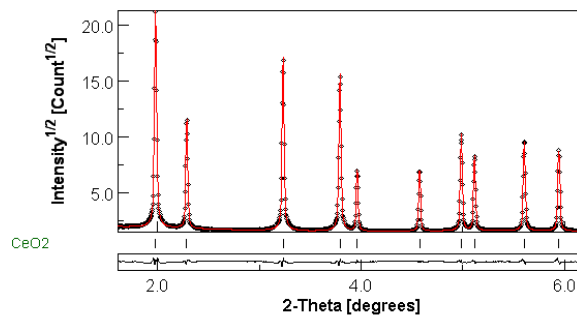


Figure 3. The Rietveld refinement results of CeO₂ using MAUD software. Black dots are the experimental data, the red line is the calculated data.

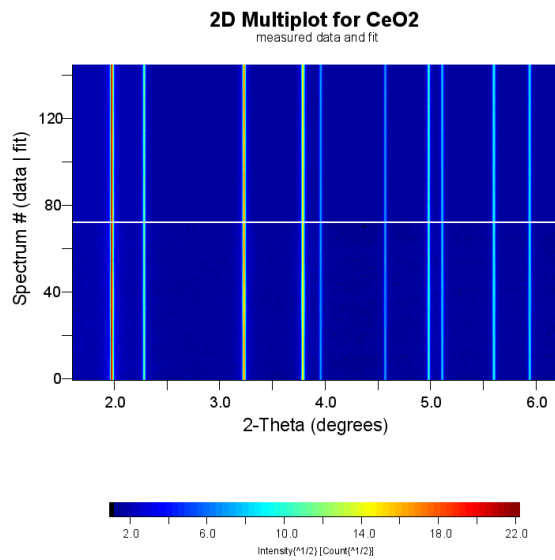


Figure 4. Stack of diffraction patterns for CeO₂ standard: Experimental data at bottom and Rietveld fitting on top.

After Rietveld refinement, good agreement in position, width and intensity between the calculated and experimental patterns was observed (Figures 3, 4), which indicate that the result is convincing (Rwp≈8%). The refined sample-to-detector distance is (1850.602±0.002) mm.

II : Texture analysis for the Nickel-coin

To perform a texture analysis, we need a sufficient number of data in order to measure a representative number of grains in different orientations. We need to cover the large part of orientation space to ensure the validity of the results.

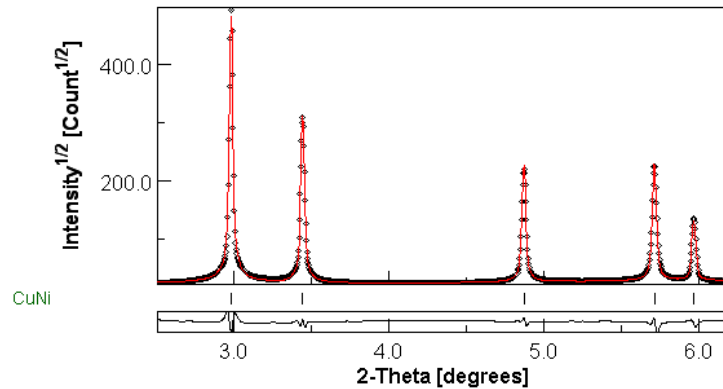


Figure 5. The Rietveld refinement of Cu-Ni coin using MAUD software. Black dots are the experimental data, the red line is the calculated data.

Rietveld refinement with the MAUD software version 2.94 was applied in order to analyze the diffraction patterns. Here and for all other samples, incident intensity, phase volume fractions (for multiphase samples), backgrounds, unit cell parameters, microstructure parameters (crystallite size and r.m.s. micro-strain in isotropic approximation), and isotropic thermal factors were refined. Texture was refined using a discrete E-WIMV algorithm.

The FCC crystal structure was considered for Cu-Ni alloy. The unit cell length refined to $a=3.59079(1) \text{ \AA}$. Figure 5 shows the results of the refinement.

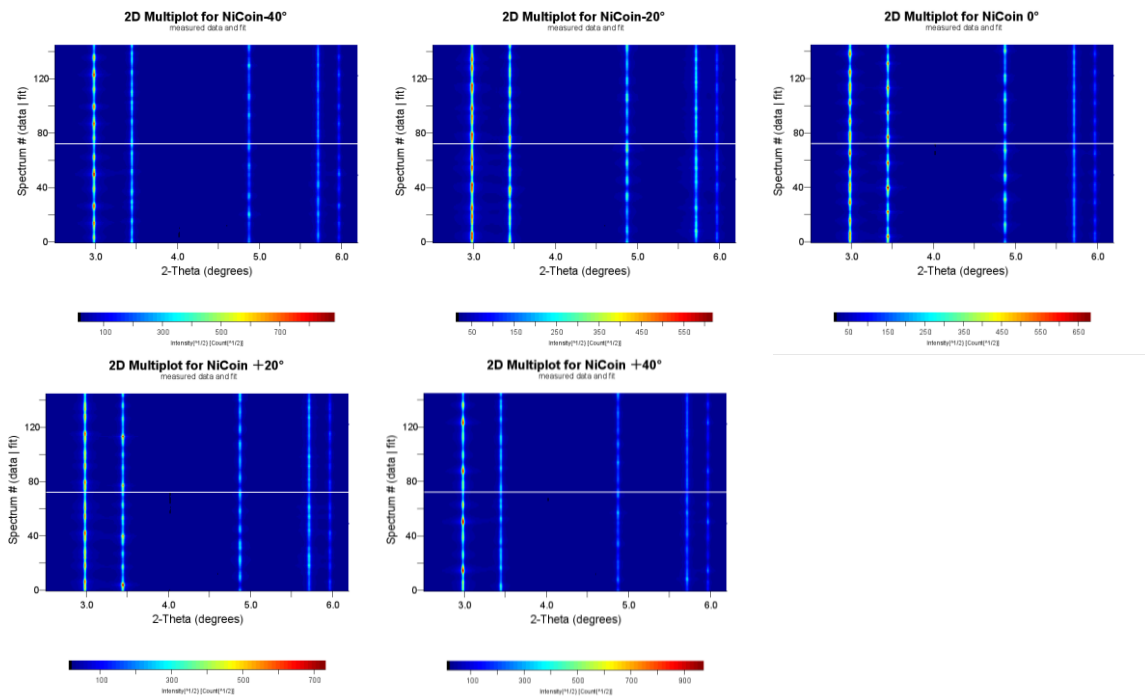


Figure 6. Stack of diffraction patterns for nickel-coin by MAUD: Experimental data at bottom and Rietveld refinement on top. (a) rotation to -40° , (b) rotation to -20° (c) rotation to 0° , (d) rotation to $+20^\circ$, (e) rotation to $+40^\circ$.

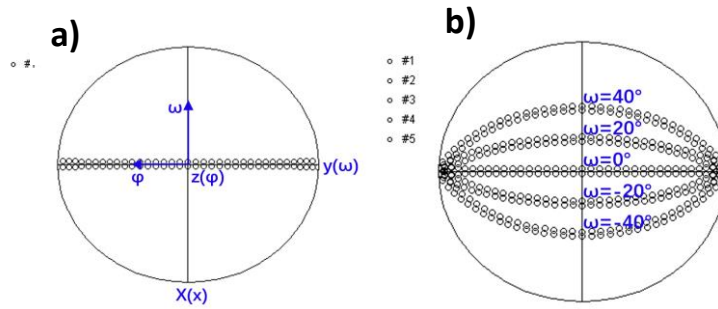


Figure 7. Pole figure coverage with a single image, demonstrating a sample coordinate system defined in MAUD (a) and with the sample rotations (b).

In order to get a sufficient data to obtain the texture pole figure results, five images are collected at $\omega = -40^\circ, -20^\circ, 0^\circ, 20^\circ$ and 40° , providing a coverage as shown in Figure 7.

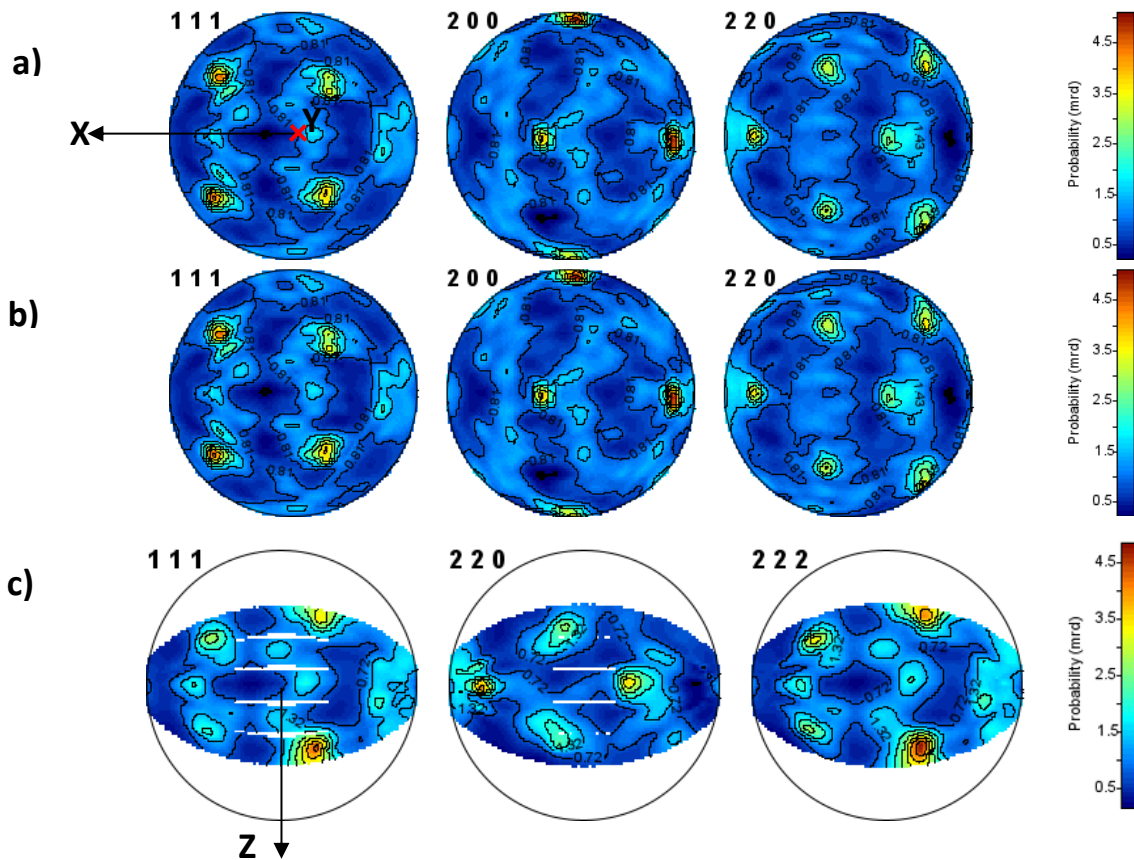


Figure 8. Plot of pole figures using MAUD software, comparing with Experimental data and different coverages. a) 1 image, 5° cell size; b) 5 images, 5° cell size; c) 5 images, 5° cell size, experimental data. Equal area projections.

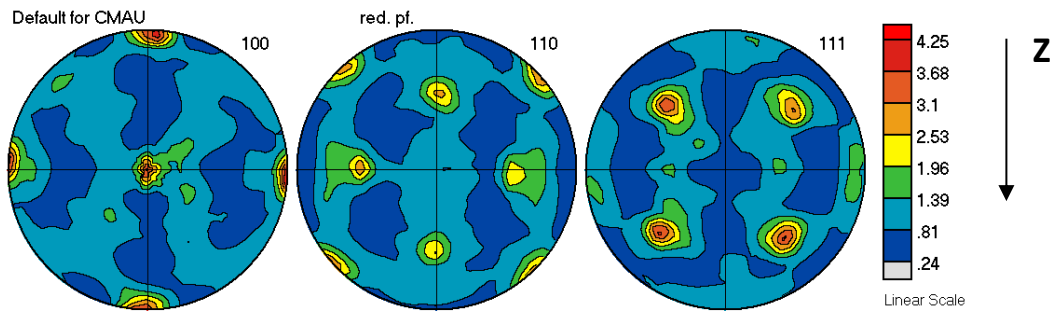


Figure 9. Plot of pole figures using MAUD software, processed with BEARTEX software: 5 images, 5° cell size. Equal area projections. Rotated -20° around Z axis to highlight the cube symmetry.

Figure 9 shows the BEARTEX-processed pole figures, showing a cube texture, which is characteristic for a recrystallized FCC metal⁷. The texture is very sharp with a texture index $F2 = 11$.

Sample 2: NiTiZr alloy

Shape memory alloys are important engineering materials. The texture of the base state of the welded as-extruded NiTiZr alloy was studied.

The experimental set-up as shown below at Figure 10. For this shape memory alloy, high-energy X-ray beam with wavelength of 0.14235 Å was used. The distance between detector and sample is about 1500mm.

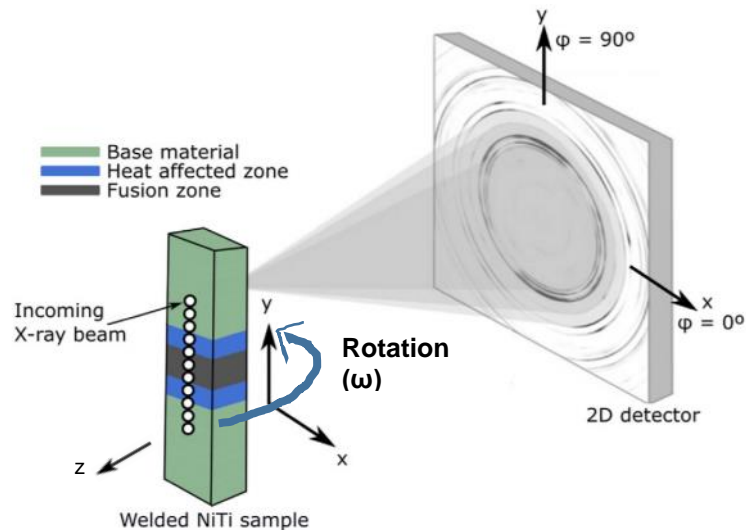


Figure 10. Experimental set-up for the X-ray diffraction experiments.

I : Instrumental Calibration

LaB₆ powder was used for the instrumental calibration.

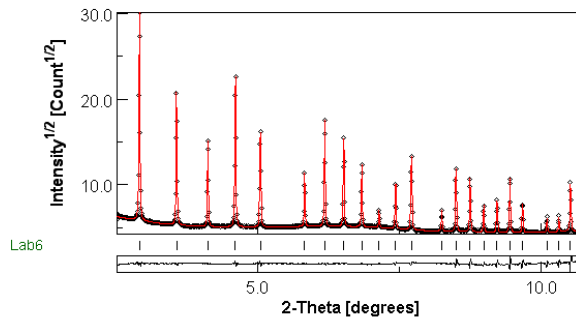


Figure 11. The Rietveld refinement results of LaB₆ using MAUD software. Black dots are the experimental data, the red line is the calculated data.

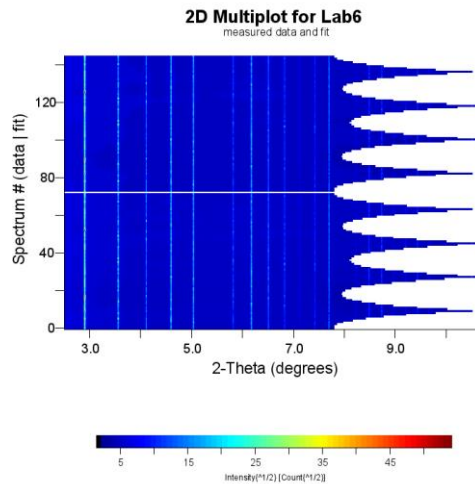


Figure 12. Stack of diffraction patterns for LaB₆ standard: Experimental data at bottom and Rietveld fit on top.

The Rwp value for the instrumental broadening refinement results shown above is around 8%, this demonstrates the reliability of the refinement model. The refined sample-to-detector distance is 1533.110±0.004mm.

II : Texture analysis for the NiTiZr alloy sample

For this analysis, 8 diffraction images were collected. It was found that the sample contains an ordered austenite phase (Pm-3m, a=3.09613(1) Å) and about 4.6Vol.% of oxide, Ni₂(Ti,Zr)₄O (Fd-3m, a=11.6769(1)Å). Due to low amount of oxide, its texture was not refined.

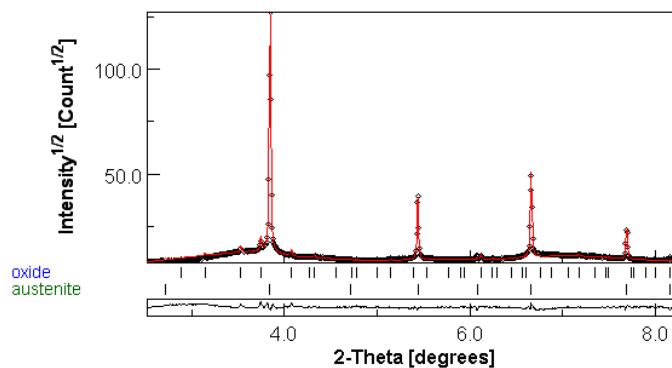


Figure 13. The Rietveld refinement results of NiTiZr using MAUD software. Black dots are the experimental data, the red line is the calculated data.

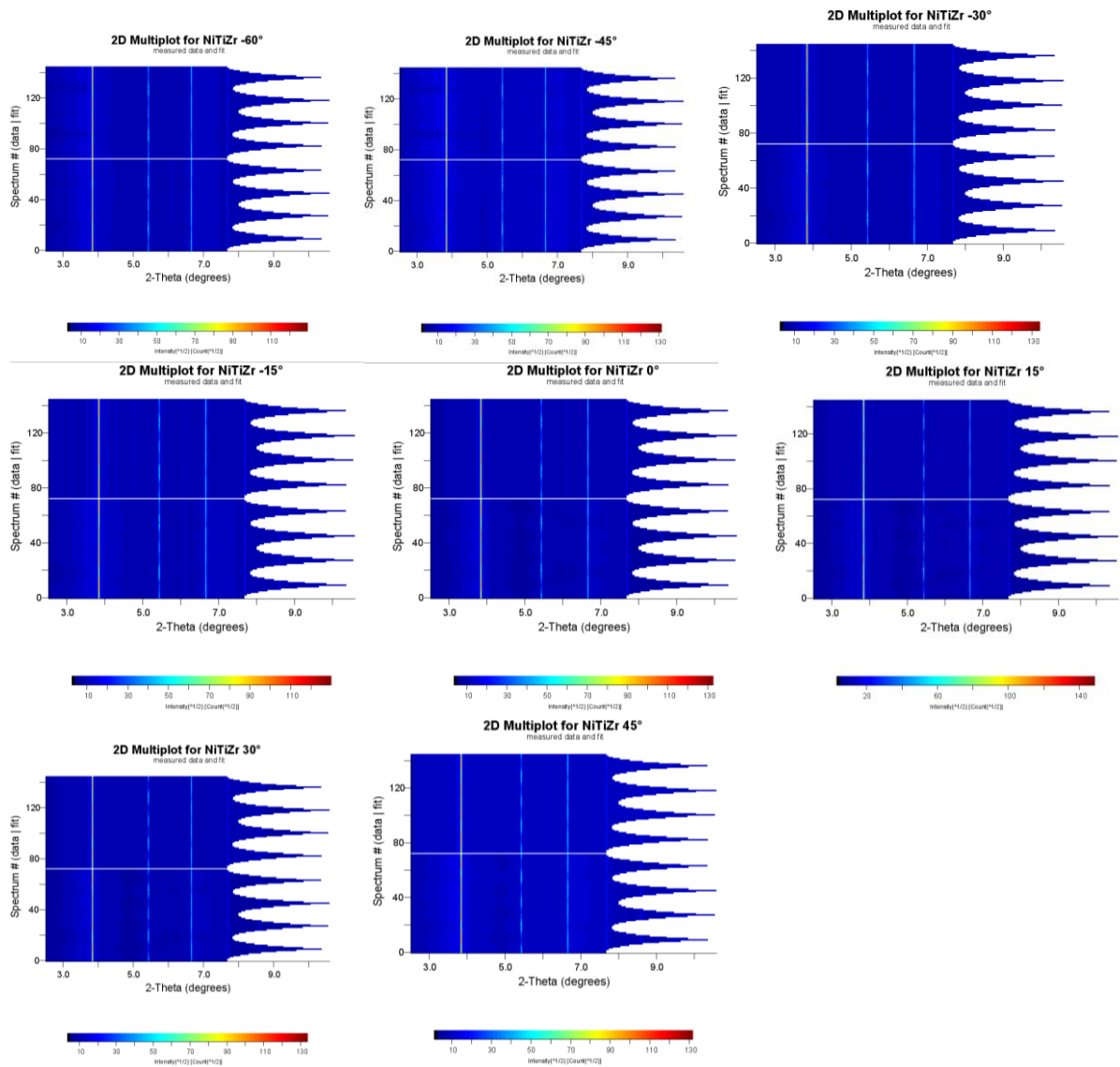


Figure 14. Stack of diffraction patterns for NiTiZr: Experimental data at bottom and Rietveld fit on top. (a) rotation to -60°; (b) rotation to -45°; (c) rotation to -30°; (d) rotation to -15°; (e) rotation to 0°; (f) rotation to 15°; (g) rotation to 30°; (h) rotation to 45°.

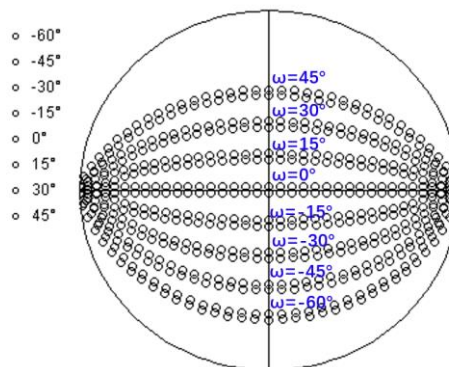


Figure 15. Pole figure coverage with the sample rotation to different positions.

In order to get a sufficient data to obtain the texture pole figure results, five images are collected at $\omega = -60^\circ, -45^\circ, -30^\circ, -15^\circ, 0^\circ, 15^\circ, 30^\circ$ and 45° , providing a coverage as shown in Figure 6.

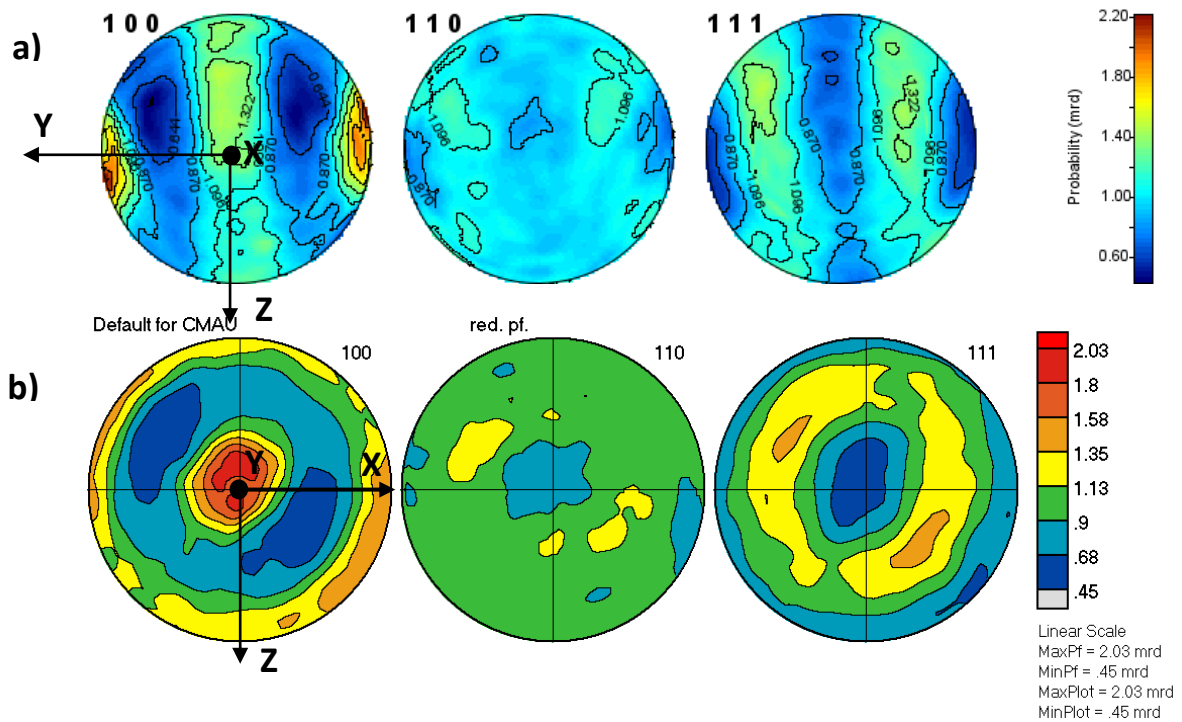


Figure 16. Plot of pole figure of austenite in NiTiZr in MAUD (a) and post-processed (smoothed and rotated) in BEARTEX software (b). Equal area projections.

Texture is close to axially symmetric. The texture is weak with a texture index of only $F2 = 1.2$.

Sample 3: High-entropy alloy (HEA)

High-entropy alloys (HEAs) are novel multicomponent alloys having five or more elements in equiatomic or near equi-atomic proportion but with simple crystal structures. Majority of the earlier investigations have focused on the alloying effect, phase transformation and properties in various HEA systems. More recently the deformation and annealing behavior of HEAs have also been studied and it is understood that appropriate thermo-mechanical treatments can enhance the properties of HEAs. But, the evolution of texture during thermo-mechanical processing with heavy deformation and annealing has not been reported so far in HEA systems. In view of future structural applications involving the HEAs, the microstructure and texture evolution during deformation and recrystallization must be understood in depth for establishing the correlation between processing parameters and mechanical properties.

I : Instrumental Broadening Determination

LaB₆ powder was used for the instrumental calibration.

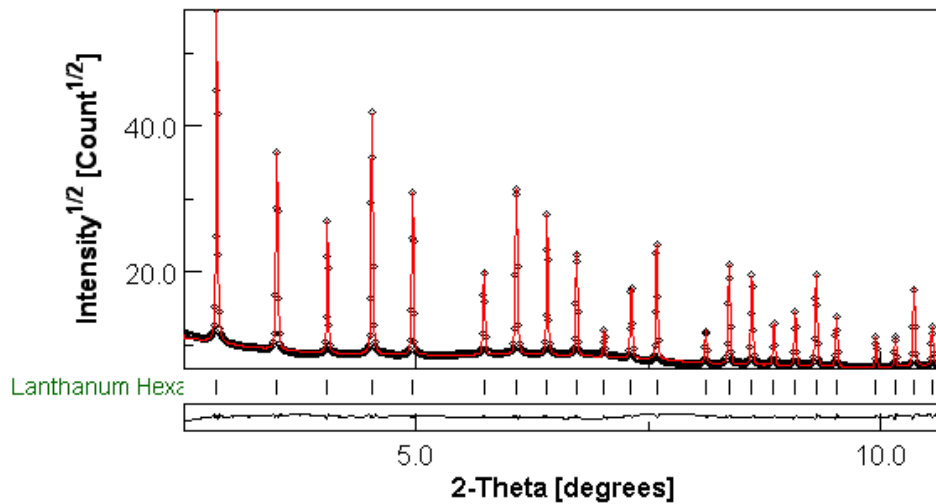


Figure 17. The Rietveld refinement results of LaB₆ using MAUD software. Black dots are the experimental data, the red line is the calculated data.

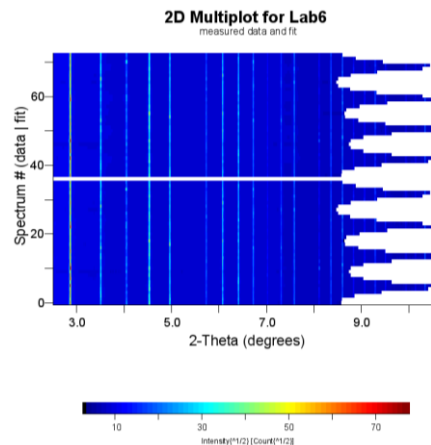


Figure 18. Stack of diffraction patterns for Lab6 standard: Experimental data at the bottom and Rietveld refinement on the top.

From above refinement results shown in the Figure 17 and Figure 18, we can see that the instrumental calibration is reasonable. The refined sample-to-detector distance is 1350.32 ± 0.02 mm.

II : Texture analysis for the HEA

The Al-Co-Cr-Fe-Ni-Ti HEA was studied in several regions: base material, heat affected zone and fusion zone (Fig. 10). Coordinate systems on all pole figure plots are the same as on Fig. 16a. It was found that in the base material region HEA is a three phase material. Phases were identified as BCC, FCC and FCC2 phases, all exhibiting a certain ordering. FCC is the most abundant phase. In heat affected zone and fusion zone, the material is a single phase FCC. There are additional diffraction peaks on all patterns that were attributed to non-textured contamination phase with hexagonal structure and unit cell parameters $a \approx 4.984 \text{ \AA}$ and $c \approx 17.039 \text{ \AA}$.

1) In the Base material region, the results are shown as below

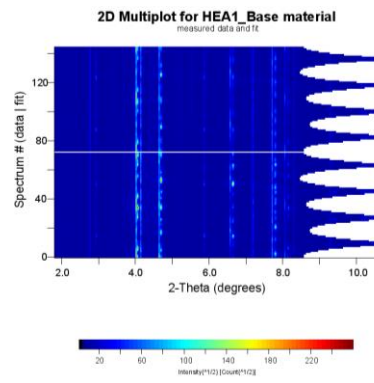


Figure 19. Stack of diffraction patterns for Base material in HEA: Experimental data at bottom and Rietveld refinement on the top.

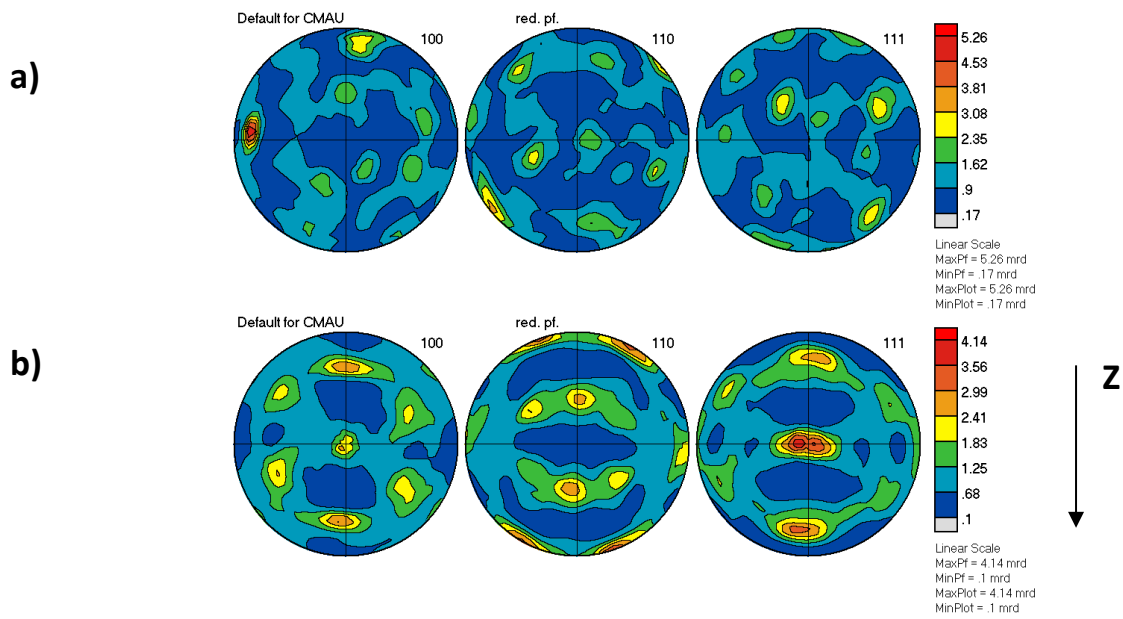


Figure 20. Plot of pole figures using BEARTEX software: a) BCC Phase; b) FCC Phase Equal area projections.

2) In the Heat affected zone, the results are shown as below

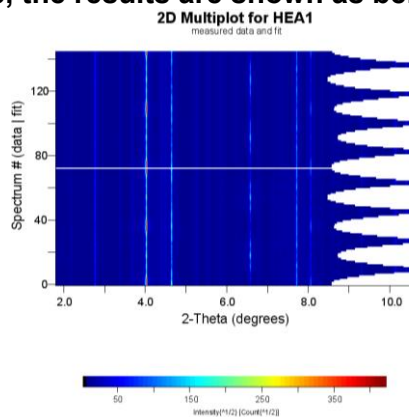


Figure 21. Stack of diffraction patterns for Heat affected zone in HEA: Experimental data at bottom and Rietveld refinement on the top.

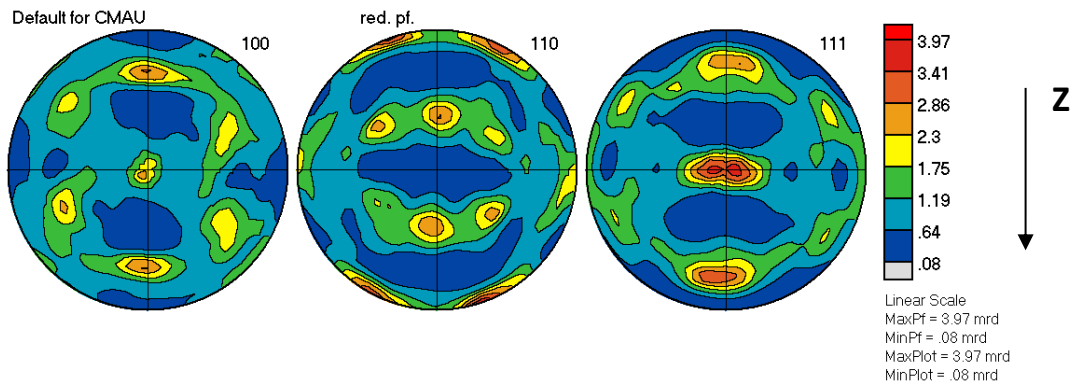


Figure 22. Plot of pole figures using BEARTEX software: FCC Phase. Equal area projections.

3) In the Fusion zone, the results are shown as below

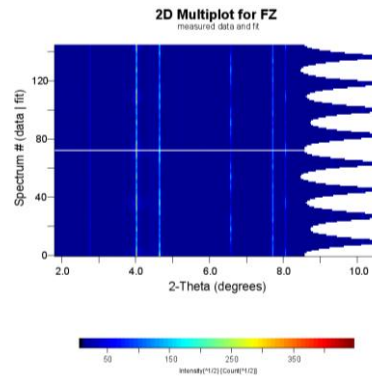


Figure 23. Stack of diffraction patterns for Fusion zone in HEA: Experimental data at bottom and Rietveld refinement on the top.

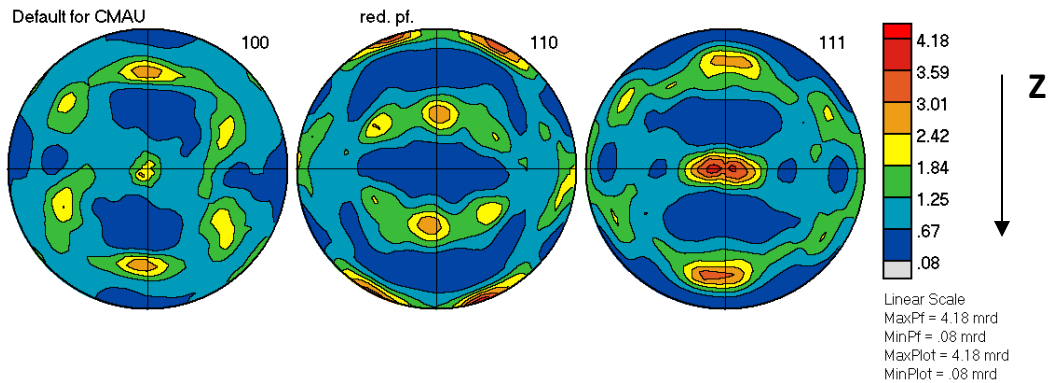


Figure 24. Plot of pole figures using BEARTEX software: FCC Phase. Equal area projections.

BCC and FCC2 phases in base material have irregular textures (e.g., Fig. 20a). The texture of FCC phase is practically independent on thermal treatment. Texture index F2 here is equal to 4.7; this indicates that the texture is rather sharp.

Conclusion

1) Application of Rietveld texture analysis to high-energy synchrotron X-ray diffraction data is a

powerful tool to study crystallographic preferred orientations in materials.

- 2) A combination of ODF calculation methods with a Rietveld method is a good solution for some cases allowing extracting additional information from diffraction pattern, such as: cell parameters, phase composition, residual stresses, etc.
- 3) Textures of crystalline phases in several alloys were studied. Phase compositions were determined for NiTiZr and high-entropy alloy.

Reference:

1. Wenk H-R, Lutterotti L, Vogel SC. Rietveld texture analysis from TOF neutron diffraction data. *Powder Diffr.* 2010;25(3):283-296. doi:10.1154/1.3479004
2. Simons H, Daniels JE, Studer AJ, Jones JL, Hoffman M. Measurement and analysis of field-induced crystallographic texture using curved position-sensitive diffraction detectors. *J Electroceramics.* 2014;32(4):283-291. doi:10.1007/s10832-014-9890-8
3. Liss K-D, Bartels A, Schreyer A, Clemens H. High-Energy X-Rays: A tool for Advanced Bulk Investigations in Materials Science and Physics. *Textures Microstruct.* 2003;35(3-4):219-252. doi:10.1080/07303300310001634952
4. Xie MY, Baimpas N, Reinhard C, Korsunsky AM. Texture analysis in cubic phase polycrystals by single exposure synchrotron X-ray diffraction. *J Appl Phys.* 2013;114(16). doi:10.1063/1.4825120
5. Rodríguez-Carvajal J. Recent advances in magnetic structure determination by neutron powder diffraction. *Phys B Phys Condens Matter.* 1993;192(1-2):55-69. doi:10.1016/0921-4526(93)90108-I
6. Lutterotti L. MAUD tutorial-instrumental broadening determination. *Departimento di Ing dei Mater Univ ...*. Published online 2006:1-18.
7. Lutterotti L., Vasin R.N., Wenk H.-R. Rietveld texture analysis from synchrotron diffraction images. I. Calibration and basic analysis. *Powder Diffraction.* 2014; 29(1). 76-84.

Acknowledgements

I would first like to thank my supervisor Dr. Roman Vasin, for being the best advisor I could have asked for in my texture analysis and Rietveld method studies. Without his expertise, guidance, strong work ethic, attention to details, and willingness to go the extra mile for me, my research goal would not have been achievable.

I would also like to thanks to my PhD supervisor Joao Pedro Olivélira. Thank him for all continued support, encouragement and guidance all the time.

Lastly and most importantly I want to thank Joint Institute for Nuclear Research. Thanks for the learning platform it gives, thanks a lot.